Journal of the Korean Geographical Society, Vol. 41, No. 2, 2006(150~167)

Fragipan Formation within Closed Depressions in Southern Wisconsin, United States

Park, S.J.*, P. Almond**, K. McSweeney***, and B. Lowery***

미국 위스콘신 남부지방의 소규모 저습지에 나타나는 이쇄반층(Fragipan)의 형성과정에 관한 연구

박수진* · 피터 알몬드** · 케빈 맥스위니*** · 벌 라우리***

Abstract : This study was conducted to determine the pedogenesis of dense subsurface horizons (denoted either Bx or Bd) observed within closed depressions and in toeslope positions at loess-covered glacial tillplains in southern Wisconsin. Some of these dense subsurface horizons, especially those occurring within depressions, show a close morphological resemblance to fragipans elsewhere, even though the existence of fragipans has not been previously reported in southern Wisconsin. The spatial occurrence of fragipans was first examined over the landscape to characterize general soil-landscape relationships. Detailed physico-chemical and micromorphological analyses were followed to investigate the development of fragipans within a closed depression along a catenary sequence. The formation of fragipans at the study site is a result of sequential processes of physical ripening and accumulation of colloidal materials. A very coarse prismatic structure with a closely packed soil matrix was formed via physical ripening processes of loess deposited in small glacial lakes and floodplains that existed soon after the retreat of the last glacier. The physically formed dense horizons became hardened by the accumulation of colloidal materials, notably amorphous Si. The accumulation intensity of amorphous Si varies with mass balance relationships, which are governed by topography and local drainage conditions. Well-developed Bx horizons evolve at closed depressions where net accumulation of amorphous Si occurs, but the collapsed layers remain as Bd horizons at other locations where soluble Si has continuously been removed downslope or downvalley. Hydromorphic processes caused by the presence of fragipans are degrading upper parts of the prisms, resulting in the formation of an eluvial fragic horizon (Ex).
Key Words : soil formation, Fragipan, wetland soils, physical ripening

요약 : 이 연구는 미국 위스콘신 남부지방의 뢰스(loess)로 덮여있는 빙퇴석평야상의 소규모 저습지와 산록부에서 관찰되는 치밀차표층(dense subsurface horizons)의 형성원인과 형성과정을 설명하기 위한 것이다. 연구대상이 된 치밀차표층은 Bd 혹은 Bx층으로 명명될 수 있는 토양층이다. 일부 치밀차표층은 형태적으로 이쇄반층(fragipan, Bx)과 매우 유사한 특징을 보이지만, 아직까지 주변 지역에서 이쇄반층의 존재가 보고된 바는 없다. 이 연구에서는 치밀차표층과 이쇄반층의 상대적인 분포의 차이를 지형기복과의 관계를 통해 관찰하였으며, 그 형성원인을 파악하기 위해 물리 · 화학적 분석과 더불어 토양구조의 현미경 관찰을 실시하였다. 그 결과 이쇄반층의 형성은 토양구조의 물리적인 숙성과정(physical ripening)과 그에 이은 콜로이드물질의 집적과정을 거치면서 형성된 것

* Corresponding author, Associate Professor, Department of Geography, Seoul National University, Seoul, Korea, catena@snu.ac.kr

** Associate Professor, Soil and Physical Sciences Group, Division of Soil Plant and Ecological Sciences, Lincoln University, Springs Road, 8150, Canterbury, New Zealand.

*** Professor, Department of Soil Science, University of Wisconsin, 1525 Observatory Drive, Madison, WI, 53706, USA.

으로 결론을 내렸다. 치밀차표층에서 관찰되는 높은 밀도의 토양매질은 빙하가 물러나면서 형성된 소규모 빙하호수와 범람원에 퇴적된 뢰스물질들이 물리적인 숙성과정(physical ripening)을 거치면서 형성된 것으로 보이며, 그 결과 대규모의 주상구조(prismatic structure)가 형성되었다. 이후 지속적인 토양화과정을 거치면서 Si를 포함하는 콜로이드 물질의 집적에 의해 토양매질이 더욱 단단해지는 과정을 거치게 되면서 이쇄반층으로 발전하게 되었다. Si의 집적정도는 지형적인 특성과 물의 흐름에 의해 결정되게 된다. 물과 물질의 집적이 주로 나타나는 소규모의 저습지에서는 Si의 집적으로 인해 잘 발달된 이쇄반층(Bx)이 발달하게 된다. 반면, Si의 제거가 비교적 활발하게 이루어지는 산록부에서는 이쇄반층의 단계로 발전하지 못하고 치밀층(Bd)에 머물고 있는 것으로 판단된다. 이쇄반층이 만들어진 경우에는 그 상부에 불투수층이 형성되어, 물리적 숙성과정으로 형성된 주상구조의 상부가 서서히 파괴되는 현상을 보기에 된다. 이 경우에는 이쇄반층 상부에 용탈이쇄반층 (eluvial fragic horizon, Ex)이 나타나게 된다.
주요어 : 토양형성작용, 이쇄반층, 습지토양, 물리적 숙성과정

1. Introduction

Fragipans are subsurface soil horizons characterized by high bulk density, slow or very slow permeability, and coarse and very coarse prismatic structures with bleached ped faces (Witty and Knox, 1989). The most typical characteristic of fragipans is the brittleness of soil fabrics at or near the field capacity (Soil Survey Staff, 1998; 1999). Air-dried soil matrices often look as if cemented, but they slake when submerged in water. Due to their dense soil matrix, plants roots could not penetrate into the prisms. Water movement is also impeded, which restricts crop growth and impairs land management (Witty and Knox, 1989).

Smeck and Ciolkosz (1989a) provide various examples of fragipans observed in USA with their possible forming processes. There appears to be no unifying hypothesis that accounts for the genesis and morphology of fragipans, but they (1989b) identified three well-respected fragipan formation theories: (1) close packing of soil matrix, (2) clay bridges, and (3) bonding by amorphous Si components. It is a compelling hypothesis that bonding agents, such as Si-rich amorphous aluminosilicates (Karanthanasis, 1987; Franzmeier *et al.*, 1989) or clay bridging (Lindo and Veneman, 1989), contribute to the brittleness of fragipans in originally unconsolidated materials (Smeck and Ciolkosz, 1989b). Such bonding theories alone, however, do not explain the development of the characteristic physical properties of fragipans, such as the very large prismatic structure and high bulk density. Bryant (1989) compared existing theories for the formation of the physical properties of fragipans. He contended that the physical ripening processes that occur during the desiccation of initially water-saturated (slurry) material could explain many of physical characteristics of fragipans.

A question that arises is the relative contribution of geochemical and physical processes to a well-developed fragic horizon. Much of the confusion related to the identification and explanation of fragipans is most likely caused by the difficulty in separating the physical properties of fragipans (high bulk density and prismatic soil structure) from the geochemical properties (the brittleness) (Bryant, 1989). After reviewing various examples, Smeck and Ciolkosz (1989b) conclude that all three mechanisms (physical ripening, clay-bridging, and bonding by

amorphous Si components) jointly contribute to the development of best-expressed fragipans, even though the dominant mechanism may differ from pedon to pedon. However, it is difficult to find previous researches addressing the relative contribution of those processes for the formation of fragipans.

In loess-covered glacial tillplains in southern Wisconsin, there are many small, closed depressions without a clearly defined drainage outlet. These closed depressions are subject to the accumulation of surface and subsurface water, forming small lakes, peat bogs, or seasonal surface ponding. Even without standing surface water, yellowish premature crops, reflecting nitrogen deficiency in the rooting zones, are an indicator of the existence of a depression. A recent hydrochemical research shows that the closed depressions may play an important role in leaching of agricultural chemicals and organic pollutants into the groundwater (Samuleson, 1999).

During pedological investigations of the soils, dense subsurface horizons, showing very large (gross) prismatic structures with brittle soil fabric, were found within the closed depression. Even though the presence of fragipans has not been reported in southern Wisconsin, they show a close morphological resemblance to fragipans elsewhere. Similar soil horizons with weak fragic characteristics (noted as Bd) are also observed at low-lying topographical positions (toeslopes and ephemeral channels). Those horizons also show well-developed gross prisms, but lack the brittleness.

This paper first presents morphological, physical and chemical evidence in support of the presence of fragipans in southern Wisconsin. We analyzed the lateral variation of soil physical and chemical properties in relation to the spatial distribution of fragipans along a toposequence. The main objective of this paper is to identify the

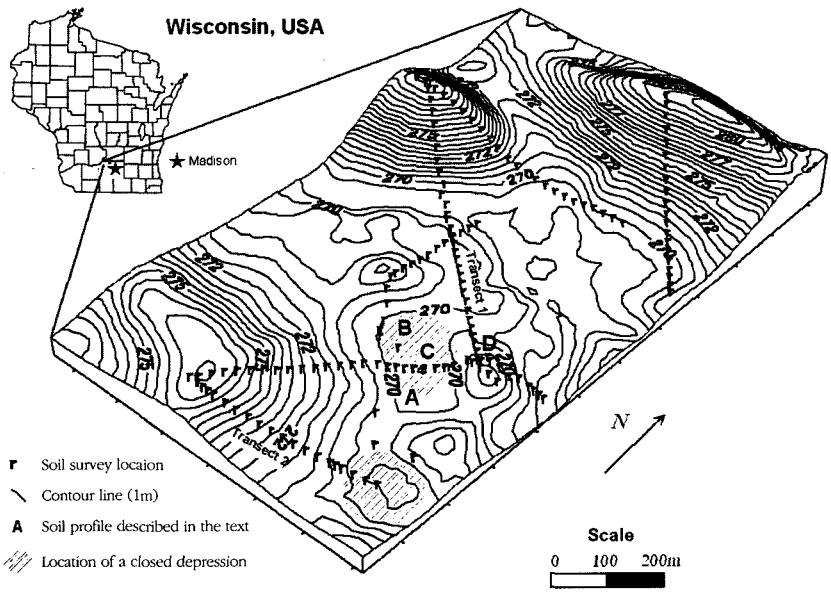

Figure 1. The study area (43.39°N, 89.38°N) at the Arlington Agricultural Research Station in southern Wisconsin.

relative contribution of physical and geochemical processes to the formation of fragipans with special emphasis on soil-landscape relationships.

2. Materials and Methods

1) Study Area

The study site is a 1.3×0.7 km area (43.39°N, 89.38°W) at the Arlington Agricultural Research Station (AARS) of the University of Wisconsin, located in Columbia County, Wisconsin (Fig. 1). The topography of the study site is gently rolling to level with some rounded hills originating from ground moraines and the surface of the underlying bedrock. Average slope angle is 2.4%, ranging from 0.0 to 15.0%. The unconsolidated glacial sediments are underlain by Ordovician and Cambrian dolomites and sandstones. The moraines date from the Lake Mills phase of the latest Wisconsinan ice advances (about 15.000 years ago). A single loess sheet up to 1.3 m thick accumulated during and after the ice retreated (Clayton and Attig, 1997). The native vegetation was tallgrass prairie, but most of the area is currently used for agricultural crops. Major grain crops are corn (*Zea Mays*), soybeans (*Glycine max.*), and wheat. The primary hay and forage crop is alfalfa (*Medicago sativa*).

The dominant soil at the study area is mapped as a Plano silt loam (fine-silty, mixed, superactive, mesic Typic Argiudolls) (Mitchell, 1978). This soil has a silt loam Ap-horizon that is 20-cm deep. The loess mantle in which the soil is forming is generally deeper than 150 cm, underlying loamy stratified outwash or sandy loam till. In some places, this soil is saturated at a depth of 90 to 150 cm for significant periods. The second most frequently found soil, the Griswold (fine-loamy, mixed, superactive, mesic Typic Argiudolls), differs from Plano in that it is found on steeper slopes and the loess layer is thinner due to erosion.

Average annual precipitation is 785 mm and mean temperature is 7.3℃. Winter temperature average is about 6.5℃ and summer temperature average is about 20℃. The soil is frozen from early December through most of March. There are no dry and wet seasons, but about 60 percent of the annual precipitation falls in the five months of May through September.

2) Occurrence of dense subsurface horizons

The occurrence of dense subsurface horizons at the study area was investigated along six soil-sampling transects from the summit to the center of valley or depressions (Fig. 1 and also see Park *et al.* (2001)). In total, 160 soils were cored using a 10 cm-diameter probe attached to a hydraulically operated soil-sampling unit. Soil morphology was described in the field, following Schoeneberger *et al.* (1998).

Sixty-one soil profiles out of a total of 160 contain various forms of dense subsurface horizons with a gross prismatic structure. Fig. 2 presents simplified soil horizonations and associated landscape positions along two slope transects. The gross prisms can be easily identified from undisturbed soil cores, showing a dense matrix with intensive hydromorphic features (gleying and iron-manganese nodules), and fine vesicular pores within the matrix. For most soil profiles, the gross prismatic structures are associated with stratified sediments of fluvial-origin, and occur in closed depressions, toeslope positions, and along ephemeral channels where short-lived channeliz-

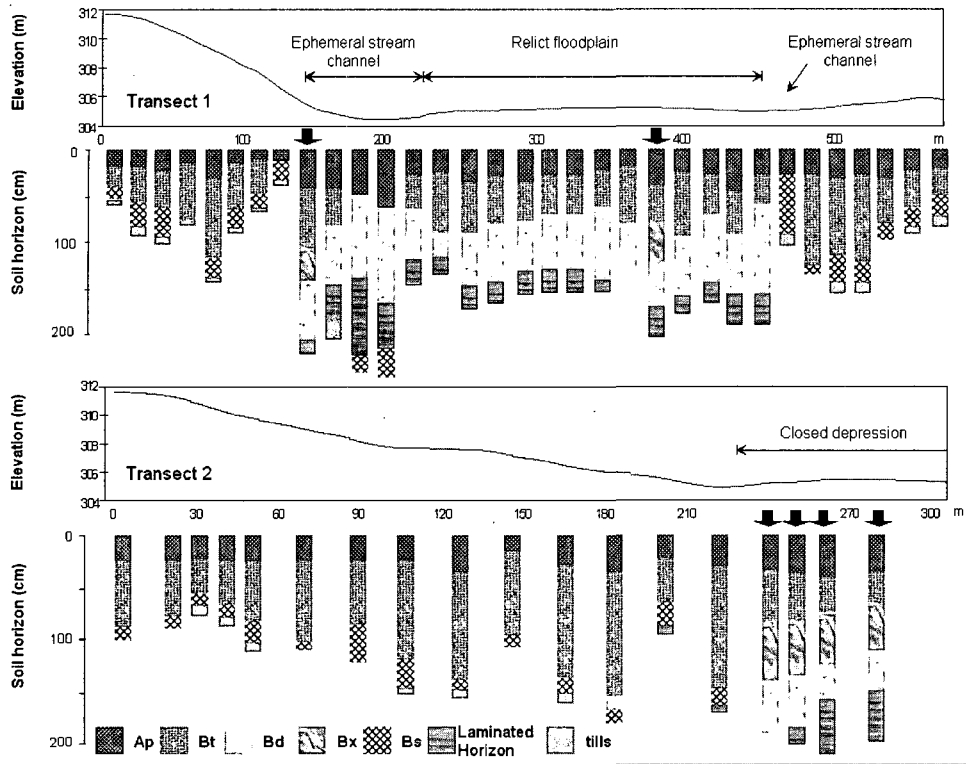

Figure 2. The change of the landscape and simplified soil horizonation along the two slope transects at the study area. The location of the transects is given in Fig. 1. The soil profiles contraining Bx horizons are marked by arrow.

ed flows occur after heavy rain.

The gross prisms are further divided into two types depending on their rupture characteristics and abundance of clay coats. The first (Bx) shows brittleness at the field capacity, while the second (Bd) shows deformable and semi-deformable ruptures. Bx horizons are generally associated with a much higher intensity of clay coats than Bd. The Bx horizons mainly occur within two relatively large closed depressions (shaded area in Fig. 1). Along transect 1 in Fig. 2, however, two Bx horizons were also observed at a footslope position and at the center of the toeslope. Both profiles show a deeper solum than adjacent soils and thick A horizons, indicating accumulation of soil materials. This indicates that the prismatic structures are widespread, but the brittleness of the soil fabric only occurs in depression areas, where water and soil materials have accumulated from the surrounding areas.

3) Field and Laboratory Analyses

Detailed morphological and pedological investigations were carried out at a closed depression where most well-developed Bx horizons were observed (transect C-D in Fig. 1). Two soil pits were excavated to 2 m depth (A and B in Fig. 1). The samples collected from genetic soil horizons were air-dried at room temperature and ground to pass a 2 mm sieve.

Bulk density was estimated using a 10×6 cm Kubiena box, and presented on an oven-dry basis. Soil pH was measured in 0.01M $CaCl_2$ solution at a 1:2 (weight: volume) ratio. Soil texture was analyzed by the hydrometer method (Gee and Bauder, 1986). Organic matter content was estimated by low-temperature loss-on-ignition (375℃) for 16 hours to prevent the weight loss by the dehydration of clays and oxides (Hesse, 1968). The content of oxides and hydroxides of Al, Fe, Si, and Mn was measured by selective dissolution techniques using acid ammonium oxalate and DCB (sodium dithionite-sodium citrate-sodium bicarbonate) solutions (Soil Survey Staff, 1984). All extracts were analyzed with Ion Coupled-Plasma Spectrophotometry at the Soil Testing Laboratory of University of Wisconsin.

Two soil blocks were collected from the Ex and Bt/2Bx horizons of the soil profile A for soil thin sections (Fig. 3). Collected soil blocks were impregnated with electric resin and duplicate thin sections were prepared following Innes and Pluth (1970). In order to investigate differences of pedogenic environment between the ped face and matrix, soil blocks were collected from the same horizons where the soil thin section samples were taken. From these blocks, coatings and bleached ped faces were carefully scraped off and separated from the matrix. DCB solution was used to extract the content of oxides and hydroxides of Al, Fe, Si and Mn from the ped face and matrix separates.

In order to identify lateral variations of soil properties along the catenary sequence, morphological and geochemical analyses were also conducted along the transect C-D (Fig. 1). Six soil pedons were examined from the local summit to the center of a closed depression (see

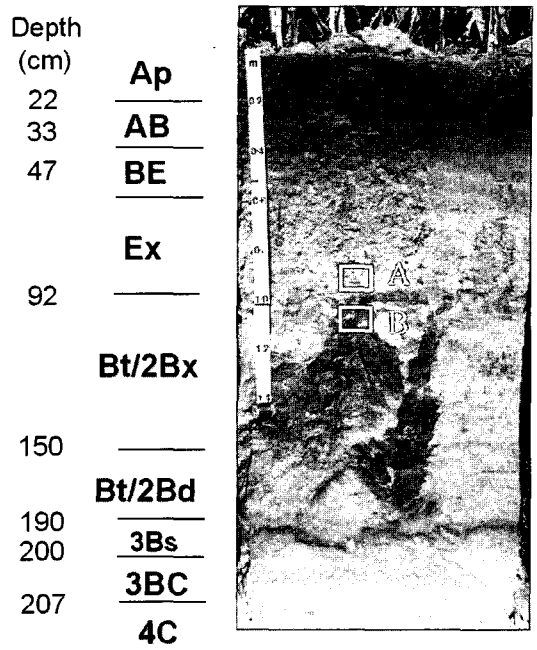

Figure 3 Photograph illustrating a representative soil profile within the closed depression (A in Fig. 1). The black boxes (A and B) indicate the locations of soil samples taken for thin section analysis.

Fig. 6). The distance between profiles was 17.5 m. At each location, duplicated samples were collected every 15 cm depth using a 7.5 cm diameter and 15 cm length soil sampler.

Even depth sampling was chosen, because the main objective of this analysis is to investigate possible lateral translocation and re-distribution patterns of soil attributes. The surveyed depth varied from 80 to 240cm, but mostly reached to tills or laminated fluvial sediments.

Soil pH, texture, organic content, and DCB and oxalate extractable oxides and hydroxides were measured as described above. Averaged values from duplicated samples for each measurement point are presented in this paper.

A non-parametric correlation analysis (Spearman's *rho*) was conducted to identify the association between soil attributes. A triangu-

Table 1. The field description of a representative soil profile (Profile A in Fig. 1) within a closed depression at the Arlington Agricultural Research Station, WI.

Horizon	Depth (cm)	Description
Ap	0 - 22	Black (7.5YR 2/1) silt loam; moderate coarse angular blocky structure breaking to moderate fine and medium subangular blocky; weak medium platy structure at the lower parts; brittle; very plastic and sticky; clear, smooth boundary AB
AB	22 - 33	Very dark grayish-brown (10YR 3/2) to dark grayish-brown (10YR 4/2) silt loam; weak platy structure to massive; brittle; moderately plastic and moderately sticky; few coarse (up to 3 mm diameter) tubular pores (earthworm holes) coated with A horizon materials; clear, wavy boundary
BE	33 - 47	Light olive brown (2.5Y 5/3) silt loam with few distinct fine yellowish red (5YR 5/6) mottles; moderate medium subangular blocky; brittle; moderately sticky and moderately plastic; the coarse tubular pores as the above; clear, wavy boundary Ex
Ex	47 - 92	Light yellowish brown (2.5Y 6/4) silty clay loam with common distinct medium strong brown (7.5YR 6/4) mottles, continuous gray (5Y 6/1) silica coating on peds; strong fine to medium angular blocky structure within gross prism; very firm; brittle; moderately sticky and moderately plastic; the coarse tubular pores as the above; abrupt, smooth boundary
Bt/2Bx	92 - 150	Yellowish brown (10YR 5/8) and grayish brown (2.5Y 5/2) silty clay loam grading to grayish brown (2.5YR 5/2) with common prominent coarse yellowish brown (10YR 5/8) mottles, yellowish brown parts is associated with black manganese (5YR 3/1) mottles, manganese mottles grading fine to coarse; strong gross (20 cm diameter) prismatic structure, upper parts breaking to strong coarse blocky structure; the face of peds are fully covered by thick dark gray (10YR 4/1) clay coatings; very firm; brittle to semi-deformable; very plastic and very sticky; no earthworm holes; diffuse, broken boundaryBt/2Bd
Bt/2Bd	150 - 196	Gray (2.5Y 6/1) silty clay loam with few fine distinct yellowish brown (10YR 5/4) mottles and strong brown (7.5YR 5/8) subhorizontal bands (up to 3 cm thick), linear and oval shape patches of dark brown (7.5YR 3/4); moderate gross prismatic structure continued from above; semi-deformable; very plastic and very sticky; sharp and wavy boundary
3Bs	196 - 200	Brown (7.5YR 4/4) to very dark brown (7.5YR 2.5/2) loam; massive; semi-deformable; illuvial sesquioxides; partly cemented; abrupt, wavy boundary3BC
3BC	200 - 207	Lamination of brownish yellow (10YR 6/6) sand and light brownish gray (2.5Y 6/2) loamy silt; convoluted layers; single grains (sandy layers) and massive (silty layers); brittle; non-sticky and non-plastic (sandy layers), slightly sticky and slightly plastic (silty layer); abrupt, wavy boundary; effervesce with 0.01M $CaCl_2$
4C	207 -	Brown (7.5YR 5/4) gravely sandy loam; massive; brittle; slightly sticky and slightly plastic

lation linear interpolation was applied to visualize lateral distribution patterns of soil attributes along the catena.

3. RESULTS

1) Soil Morphology

Fig. 3 and Table 1 describe the morphology of the soil profile A (Fig. 1). The morphology and

physico-chemical soil attributes of dense subsurface horizons well match to the current definition of fragipans (Soil Survey Staff, 1998; 1999). The fragipans are dense, with a strongly developed, very coarse prismatic structure (denoted Ex and Bt/2Bx) (Fig. 3). The diameter of prisms reaches 30 cm. The tops of the prisms are about 50 cm from the soil surface. The prismatic structure extends as deep as 2 m into the underlying stratified sediments, although structural development is weaker below 150 cm depth (Bt/2Bd).

The Ex and Bt/2Bx horizon has firm or very firm soil strength and brittle rupture in field conditions, whereas the Bt/2Bd horizon is firm with brittle to semi-deformable failure with higher water content than Bt/2Bx. The matrix of prisms contains fine platy structures and very many fine vesicular pores. Roots are absent except along prism faces and within large pores generated by earthworms. The soil matrix shows intense redoximorphic features including a gleyed soil matrix with many fine prominent black iron-manganese concretions.

Dark-colored clay-humus coatings occur on ped faces of the Bt/2Bx and Bt/2Bd horizons. The clay-humus coats fill most of the gaps between prisms, and also some vesicular pores in the upper parts of Bt/2Bx horizon. In contrast, the Ex horizon shows a high intensity of bleaching along ped faces. The primary soil structure of the Ex horizon is gross prism, but with strongly developed subangular blocky structure as a secondary soil structure. Albic characteristics are further extended to the overlying BE horizon.

One common characteristic of soils associated with gross prisms is the presence of stratified soil materials at the lower parts of the prisms (denoted Bt/2Bd for profile A). The alteration of different soil-textural layers indicates the presence of active fluvial processes during its deposition. The Bt/2Bd horizon is connected to coarser (sand and loamy silt) stratified sediments (3BC) overlying glacial tills (4C). The 3BC horizon shows convolution features that might have been formed by cryoturbation under the periglacial environment. A thin, partly cemented, Bs horizon (3Bs) is observed between the stratified sediments and overlying loess. The presence of a Bs horizon is a reliable indicator of free carbonates immediately below. The abrupt change of hydraulic characteristics between loess materials and tills might have caused the deposition of illuvial soil materials from above.

2) Soil Properties and Micromorphology

The Ex and Bt/2Bx horizons have higher bulk density (1.43 g/cm^3 in the Ex horizon and 1.62 g/cm^3 in the Bt/2Bx horizon) than overlying and underlying horizons (Table 2). Soil thin sections show that the close packing of grains is the main cause of the high density in these horizons (Fig. 4). Clay content increases from around 25% in the A horizon to a maximum of 34% in the upper part of Bt/2Bx horizon. Overall, the Ex horizon has higher clay content than other horizons except Bt/2Bx. The thin sections show that the Ex horizon contains abundant clay within matrix and pores, but clay coats show degrading patterns (Fig. 4). The majority of coats exist as pocket shapes at both ped faces and the wall of pores. In contrast, the Bt/2Bx horizon has well-developed, thick clay coats on ped faces and in pores.

The concentration of DCB extractable Fe (Fe_d) is greater in the Ex horizon than in the underlying Bt/2Bx horizon. The ratio between

Table 2. Selected physical and chemical properties of Profile A (Fig. 3 and Table 1).

Depth	Soil horizon	Bulk density	pH	Los-on -Ignition	Sand	Silt	Clay	DCB extractable oxides and hydroxides (g/kg)				Oxalate extractable oxides and hydroxides (g/kg)				Fe_o/Fe_d	Si_d/Al_d
(cm)		(g/cm^3)		(%)	(%)	(%)	(%)	Al	Fe	Mn	Si	Al	Fe	Mn	Si		
0-20	Ap	1.17	5.99	5.57	5.71	69.78	24.51	0.76	6.98	0.75	0.38	1.28	3.93	0.74	0.27	0.56	0.50
20-32	AB	1.22	5.00	3.99	3.70	72.37	23.94	1.30	7.26	0.42	0.28	1.65	4.57	0.41	0.18	0.63	0.22
32-52	BE	1.23	4.34	2.47	1.95	74.33	23.73	0.98	8.45	0.42	0.30	1.23	5.21	0.33	0.18	0.62	0.31
52-62	Ex1	1.33	4.26	2.31	4.05	64.01	31.94	1.09	9.01	0.52	0.41	1.51	5.85	0.44	0.27	0.65	0.38
62-87	Ex2	1.52	4.54	2.18	3.52	64.66	31.82	1.02	10.33	0.71	0.38	1.39	5.68	0.68	0.24	0.55	0.37
87-107	Bt/2Bx1	1.58	4.85	2.02	2.96	63.13	33.91	0.87	8.63	0.72	0.42	1.38	5.04	0.70	0.29	0.58	0.48
107-127	Bt/2Bx2	1.63	5.12	1.88	2.32	67.51	30.17	0.55	6.46	0.66	0.41	1.15	4.30	0.84	0.34	0.67	0.75
127-147	Bt/2Bx3	1.63	5.32	1.36	3.33	69.46	27.21	0.43	4.92	0.74	0.50	1.05	3.57	0.78	0.23	0.73	1.16
147-167	Bt/2Bd1	1.59	5.43	1.38	7.08	69.89	23.03	0.44	8.46	0.39	0.51	0.83	3.98	0.42	0.31	0.47	1.16
167-185	Bt/2Bd2	1.51	5.62	1.27	13.14	65.92	20.94	0.30	4.6	0.28	0.47	0.72	2.94	0.33	0.30	0.63	1.57
185-192	Bt/2Bd3	1.49	5.81	1.22	30.28	53.81	15.91	0.22	8.97	0.83	0.35	0.79	10.81	1.38	0.97	1.21	1.59
192-200	3Bs	1.71	6.30	0.58	41.80	45.71	12.49	0.23	5.75	0.39	0.51	0.56	3.51	0.42	0.41	0.61	2.22
200-210	3BC	1.67	6.51	0.50	57.95	32.19	9.87	0.19	4.65	0.22	0.36	0.33	1.63	0.16	0.21	0.35	1.89
mean		1.54	5.31	2.06	13.68	62.52	23.81	0.64	7.27	0.54	0.41	1.07	4.69	0.59	0.32	0.65	0.64

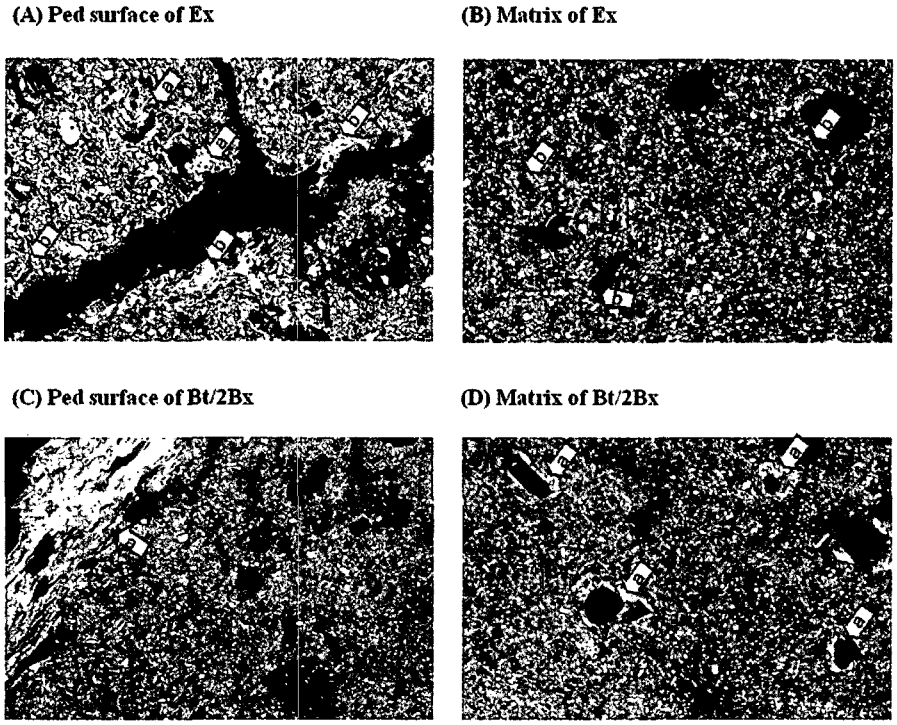

Figure 4 Soil thin section showing the ped face and matrix of Ex and Bt/2Bx horizons. Under a plane polarized light, and the scale is not known. The arrows with letter 'a' indicate well developed layered clay coats, but the arrows with letter 'b' show degraded clay coats. The degraded clay coats exist as 'pocket shape' on the faces of void or ped surface. The arrow with letter 'c' shows a bright brownish iron accumulation within the matrix.

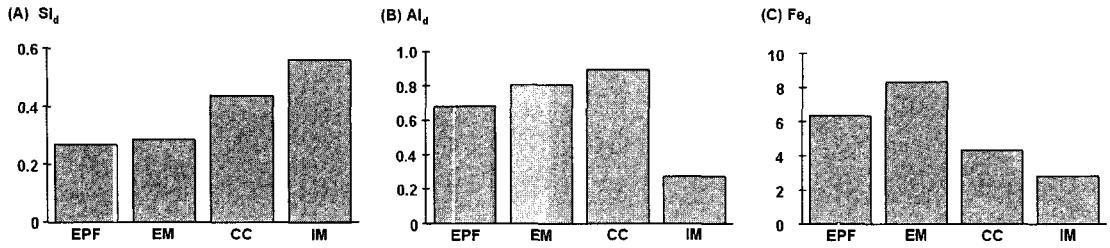

Figure 5 DCB extractable oxides and hydroxides at the Ex and Bx/Bt horizons. EPF = Eluvial Ped Face (Ped surface of Ex), EM = Eluvial Matrix (Matrix of Ex), IM = Illuvial Matrix (Ped surface of Bt/2Bx), and CC = clay coats (Matrix of Bt/2Bx).

oxalate extractable Fe (Fe_o) and Fe_d indicates that Fe oxides in the Ex horizon are relatively well crystallized (low Fe_o/Fe_d). On the other hand, Fe in Bt/2Bx is relatively poorly crystallized (high Fe_o/Fe_d). Park and Burt (1999) showed that Fe_o/Fe_d is a good indicator showing the duration of water saturation over the landscape. The vertical function of Fe_o/Fe_d indicates that water saturation is more persistent in the Bt/2Bx horizon, but more frequent alternation of oxidation-reduction occurs within the Ex horizon. This observation was also confirmed from soil thin sections, showing that matrix and clay coats in the Ex horizon contain higher amounts of brownish color Fe oxides than those in the Bt/2Bx horizon (Fig. 4).

Amorphous Si (Si_d) has a special significance for the formation of fragipans. Many investigators report the elevated levels of amorphous Si in fragipans and hypothesize that free silica or amorphous aluminosilicates are responsible for the brittleness of the soil matrix (see Franzmeier *et al.*, 1989; Karathanasis, 1989). The amount of Si_d tends to increase from the Ex horizon and reaches its maximum in the Bt/2Bx horizon (Table 2). DCB-extractable Si shows a concordant increase with the bulk density of subsurface soils. In a correlation analysis, however, Si_d is independent of the vertical distribution of clay (*rho* = -0.01), while oxides and hydroxides of Fe_d and Al_d correlate positively with clay (*rho* = 0.68 with Al_d; 0.82 with Al_o, and 0.51 with Fe_d). Similar findings are reported by Harlan and Franzmeier (1977), Steinhardt and Franzmeier (1979), and Norton (1986). The ratio between DCB extractable Si and Al progressively increases with depth; this is mainly caused by decrease in Al_d with depth. The same pattern was also observed along the catena described below (Fig. 7).

In the separate measurement of DCB extractable elements from eluvial ped face, eluvial matrix, illuvial matrix, and clay coat (Fig. 5), Si_d shows a high level in both the illuvial matrix and clay coats from the Bt/2Bx horizon. While clay coats contain large amounts of Al_d, the matrix of the Bt/2Bx horizon shows a much lower content of Al_d than those in the eluvial matrix and ped face from the Ex horizon. The content of Fe oxides in the clay coats and illuvial matrix of the soil is much lower than eluvial parts of the soil, reflecting active redoximorphic processes within the Bt/2Bx horizon or limited translocation from the above.

3) Catenary Soil Development

The relief along the sampling transect C-D is less than 1 m over a 70 m distance, but soil

morphology varies markedly (Fig. 6(A)). Soil depth to till is thin in upslope positions (profiles 2-4 and 3-5), and then abruptly increases from profile 4-6 where stratified glacio-fluvial sediments and Bt/2Bx horizons appear. Depth to stratified sediments at profile 4-6 is 151 cm, and it becomes gradually deeper from profile 5-7 (about 190 cm). The appearance of thick-clay-coated gross prisms in the subsoil coincides with profile 5-7. The soil survey around transects C-D showed that stratified sediments and gross prisms only occur within a closed depression approximately 180 m in diameter (see Fig. 1). The increase of the thickness of A horizons within the depression is due to active deposition of soil materials from upslope.

Bulk density variation along the transect C-D is shown in Fig. 6 (B). Bulk density is relatively high (>1.60 g/cm^3) in three locations: 1) in topsoils in the upper slope, which may be caused by soil compaction, 2) within the boundary between loess materials and tills at upper slope soils where translocated clays and sesquioxides partly cement soil matrices, and 3) in the Bt/2Bx horizons within the closed depression. A progressive increase of bulk density toward the center of the depression is also clearly shown.

In the correlation analysis for all soil samples from transect C-D, bulk density shows a moderate negative correlation with organic matter content (*rho* = -0.61) and Al_d (*rho* = -0.51),

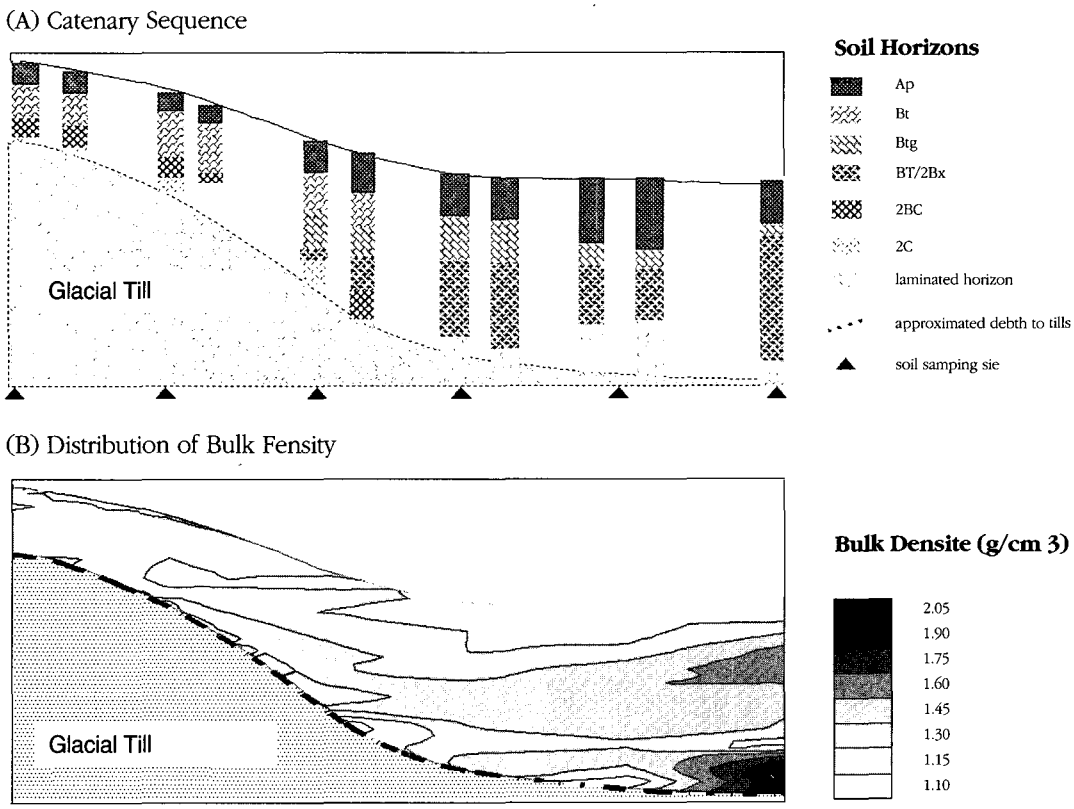

Figure 6 Soil morphology and bulk density distribution along the slope transect B–C.

Table 3. Spearman's *rho* between measured soil attributes along slope transects A–B (n=74).

	Bulk density	Organic content	Soil pH	Clay content	Si_d	Fe_d	Mn_d	Al_d
Bulk density	1.000							
organic conten	-0.610**	1.000						
Soil pH	-0.132	-0.006	1.000					
Clay content	-0.149	0.556**	-0.119	1.000				
Si_d	0.491**	-0.383**	0.416**	-0.008	1.000			
Fe_d	-0.258*	0.158	0.112	0.033	-0.101	1.000		
Mn_d	-0.096	0.070	0.225*	0.049	0.169	0.624**	1.000	
Al_d	-0.510*	0.636**	-0.483**	0.293**	-0.698**	0.305**	-0.040	1.000

** Correlation is significant at the .01 level (2-tailed).

* Correlation is significant at the .05 level (2-tailed).

but a moderate positive correlation with Si_d (*rho* = 0.49). No significant correlation was observed between bulk density and clay content. There is a progressive increase of Si_d in the subsurface soil horizons towards the center of the depression, and the close association of Si_d with bulk density is clear in Fig. 7 (B) and Fig. 6 (B). On the other hand, Fe_d indicates depletion of Fe

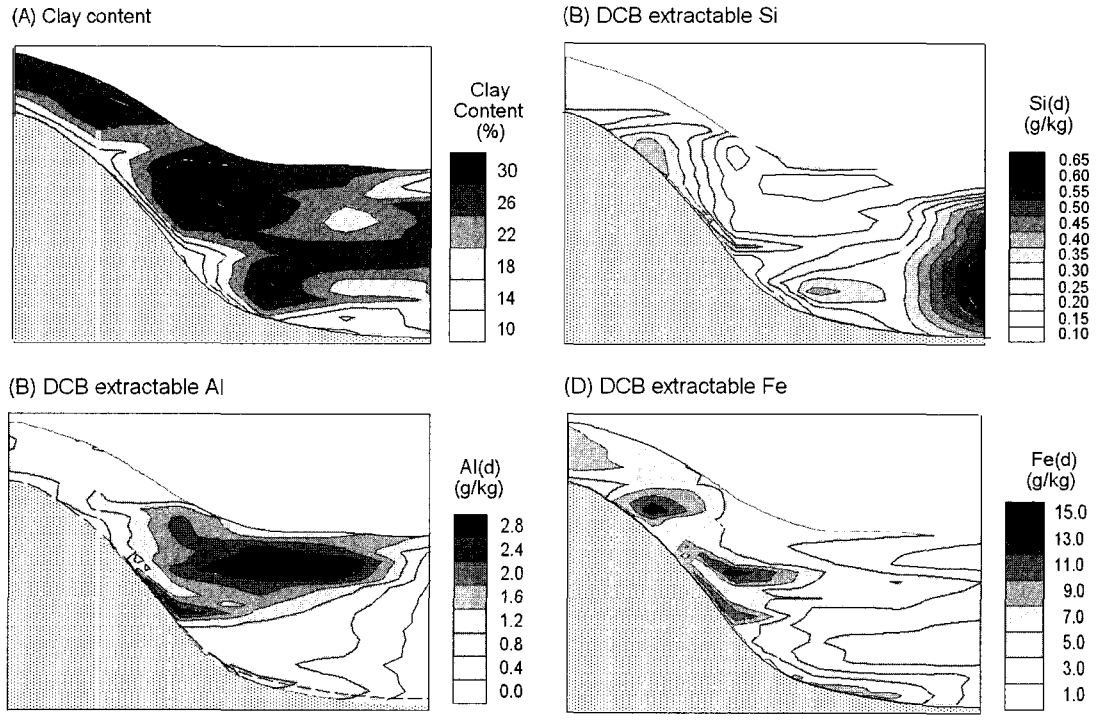

Figure 7 Catenary development of soil attributes. (A) Clay content; (B) DCB extractable Si; (C) DCB extractable Al, and (D) DCB extractable Fe. Triangulation with linear interpolation along the transect.

oxides from the highly gleyed soils within the depression (Fig. 7 (D)).

There is high negative correlation between Si_d and Al_d (*rho* = -0.70), which is well presented in a comparison between Fig. 7 (B) and 7 (C). Unlike Si_d, high levels of Al_d occur in the topsoils of the closed depression and footslope positions. A detailed mineralogical investigation of Al_d and Si_d is beyond the scope of this research, but the data indicate different mobility of Al and Si along the catenary sequence. It is generally believed that Al released by mineral weathering forms various hydroxides, which are mobilized by certain organic components except in a very acid soil environment (Franzmeier *et al.*, 1989). The relative high correlation coefficient (*rho* = 0.64) between Al_d and organic matter is indicative of the role of organic materials in Al mobilization. On the other hand, Si is freely moved as silicic acid (H_4SiO_4) independent of organic materials and clay (Karathanasis, 1989). The higher Al_d level in clay coats than in the matrix of the Bt/2Bx horizon (Fig. 5 (B)) suggests that Al may be translocated into the illuvial zones (Bt/2Bx) as Al-organic complexes and deposited on ped faces. Unlike Al, however, soluble Si can penetrate into the dense matrix and may accumulate within matrices as either amorphous silica or aluminosilicates.

4. Discussion

1) Formation of prismatic structures

From soil morphologies, the following sequences of sedimentological and pedological histories can be inferred site: 1) the deposition of glacial tills (4C in profile A); 2) the deposition of glacio-fluvial sediments under a periglacial environment (3BC in profile A); 3) the deposition of stratified silt-loamy, silt layers originating from loess and fluvial sediments; 4) continuous deposition of loess covering the stratified sediments; 5) the formation of gross prisms, possibly during continuous depositions of loess, and 6) Holocene pedogenesis associated with the formation of Ex and Bt/2Bx horizons. The first four processes are concordant with environmental changes related to the retreat of the last glacier and loess depositions in southern Wisconsin (Clayton and Attig, 1997).

The formation of coarse prismatic structures from a uniform, silty lacustrine sediment has been described by Jha and Cline (1963) in New York. They observed that the prismatic structure and dense fabric formed via repeated desiccation processes soon after deposition and persisted throughout the subsequent course of pedogenesis. Bryant (1989, p.147) elaborated on this process, proposing three successive steps involved in the formation of dense, very coarse prismatic structure in soils: (1) the formation of collapsible sediments; (2) the process of collapse that occurs when intergranular bond strength is reduced at saturated and near saturated condition; (3) the desiccation process following collapse cause cracking and formation of prismatic structure. The latter is referred to as a physical ripening process. Recently Assallay *et al.* (1998) further developed the collapse theory for the fragipan development in loess soils.

These collapse and subsequent desiccation processes are well-supported by field observations in our study. During the retreat of the glacier in late Wisconsin times, low-lying slope positions were subjected to frequent

flooding and fluvial processes (Clayton and Attig, 1997). Most soils containing gross prisms are closely associated with silty loess or stratified layers of silt-loamy and silt that were formed in water-saturated environment. Such depositional environment is one of the most favorable conditions for self-weight collapse of soil materials (Bryant, 1989). After complete disappearance of ice from the landscape, a change to a drier climate took place in the early Holocene. The transition from a wet to a drier climate might have initiated desiccation processes after the collapse of soils. The abundant vesicular pores and fine platy structures observed within the matrices of coarse prisms may be also indicative of the collapse of slurry materials. It is widely believed that vesicular pores are evidence of a soil material that has behaved as a liquid at some time (Habecker *et al.*, 1990).

2) Accumulation of amorphous silica within the closed depression

Franzmeier *et al.* (1989) present a model to explain the elevated Si_d content in fragipans developed in loess in the midwestern USA. According to their model, silicate minerals weathered under acid conditions release silicic acid (H_4SiO_4), which is leached to lower horizons in solution. Silicic acid accumulates in the fragipan and becomes absorbed on surfaces as either as free silica or as an aluminosilicate when water in the fragipan becomes supersaturated due to the transpiration of water by plants and evaporation. Karathanasis (1987) observed that the solutions collected in fragipans in Kentucky were at or near saturation with respect to amorphous SiO_2. Based on thermodynamic relationships, he argued that the weak cementation of fragipans occurs as a result of either amorphous SiO_2 or highly siliceous amorphous materials accumulated between particles and within pores. Irreversible precipitation of amorphous SiO_2 on the aluminosilicate coating of soil particles via dehydration could bridge and bond particles.

The high level of Si_d in Ex and Bx horizons of soil profile A indicates the presence of amorphous silica as geochemical bonding agents. At the same time, the progressive increase of Si_d towards the center of the closed depression shows that the accumulation of amorphous Si is governed by topographic conditions. The dissolved Si weathered from mineral weathering flow into the closed depression from the surrounding landscape. Due to the limited outflux of silicic acid from depressions, the soil solution will be easily saturated. As shown in the comparison of the coats and matrix from the Bt/Bx horizon (Fig. 5), silicic acid could penetrate into the dense matrices of prisms and precipitate as amorphous silica or aluminosilicate via dehydration. The lack of brittleness in the Bt/2Bd horizon, despite the relatively high Si_d content, may be caused by long-lasting water saturation, which is not favorable for the precipitation of soluble silica within the soil matrices.

In floodplains or channels, however, silicic acid passing through with subsurface lateral water and precipitation within the soil matrix could be limited. Consequently, subsurface horizons, although dense, do not develop the hardening and brittle failure of their counterparts in the closed depressions. The importance of drainage conditions for well-developed fragipans has also been hypothesized in previous research (Nettleton *et al.*, 1968; Franzmeier *et al.*, 1989).

Karanthanasis (1989) further developed the idea that the supersaturation of silica occurs at certain landscape positions due to the influx-outflux balance of the soil system and drainage characteristics.

Although clay bridging as a binding agent was not specifically tested in this research, the contribution of clay bridging to the brittleness seems relatively small. The illuviated clays are mostly deposited both on the surface of prisms and within the pores, and could not penetrate into the dense soil matrix. The clay-bridging theory was mostly evidenced by the fragipans in rather coarse soil materials, such as glacial tills and sandy materials (Lindo and Veneman, 1989). The silty loess with an already dense soil matrix is not a likely condition for the bridging of soil particles by illuviated clays.

It is interesting to consider the temporal relationship between the development of prismatic structure and silica accumulation in a fragipan. The first is the result of a physical process over a short time span at the earliest phase of soil development, whereas the second takes place as a progressive process related to weathering of soil materials and catenary accumulation. Generalizing these observations, we could expect that the existence of low permeability horizons at an appropriate depth may be a necessary condition for the accumulation of amorphous silica and other binding agents. Such subsurface impermeable horizons may also include heterogeneity of parent materials, presence of paleosols, glacial compaction, permafrost actions, physical ripening and desiccation processes (Bryant, 1989). On the other hand, the presence or absence of binding agents depends on the geochemical environment and mass-balance relationships over the landscape.

3) Formation of Ex horizons

One of most active contemporary processes associated with the fragipans might be the formation of the Ex horizon. This horizon is a zone of degradation of the gross prism under the influence of episaturation above the Bt/2Bx horizon. The presence of dense subsurface layers may significantly reduce the hydraulic conductivity of soils resulting in the formation of a perched water table. The accumulation of clays between the gaps of prisms and the progressive development of Bx horizons may further increase episaturation within the depressions.

Hydromorphic processes, including ferrolysis, caused by seasonal episaturation have been implicated in other studies reporting degradation of argillic horizons that overlie fragipans (Ray, 1967; Bullock *et al.*, 1974; Miller *et al.*, 1993; McDaniel and Falen, 1994). Bullock *et al.* (1974) reported similar morphological features: bleached albic ped faces over a fragipan with thick clay coats in the Udalfs of New York State. They concluded that most of the clays in the lower illuvial horizons have been translocated from above with limited neoformation in place. During a pedogenic investigation of an eluvial fragipan in northern Minnesota, Miller *et al.* (1993) inferred that Ex horizons were thickening at the expense of underlying Btd horizons due to water saturation. During seasonal or periodic episaturation, clays may be removed from the bleached E horizon (and also from A and BE horizons) and move further down into Bt/2Bx.

It is likely that similar processes are occurring in our study area. The soil thin section analyses support the idea that the Ex horizon retains a number of relict features (high clay content, prismatic structure, degraded clay coats) that are

being progressively destroyed by a new phase of pedogenesis (Fig. 4). The frequently alternating wetting and drying cycles at the upper parts of the prism may also be responsible for the formation of the secondary blocky structure of the gross prisms.

5. Conclusion

The dense subsurface horizons observed within closed depressions in southern Wisconsin satisfy the morphological criteria of current definitions of fragipans. Fragipan formation at the study area took place in two stages. The first, described as a physical ripening process, involves the formation of a dense horizon with a close-packed fabric through the collapse and desiccation of an initially water-saturated silty sediment. During the retreat of the last Wisconsinan glacier, the prismatic structure formed from saturated sediments accumulated in closed depressions and toeslope positions. The second stage involves hardening of the dense horizon and development of brittle failure, which is caused by the progressive accumulation of amorphous siliceous minerals within soil matrices. In closed depressions that have no clear outflux for transported soil materials from the surrounding area, soluble silica accumulated within depressions precipitates as amorphous silica or aluminosilicate minerals within the matrix. In other locations, soluble silica passes through with the subsurface lateral water flow and does not accumulate. Consequently, subsurface horizons, although dense, do not develop the brittle failure of their counterparts in the closed depressions. The progressive development of Bx horizons may further reduce the hydraulic conductivity of the fragipans. Hydromorphic processes caused by seasonal episaturation are degrading the upper parts of the gross prism, forming eluvial fragipans (Ex).

Acknowledgements

This research has been supported by the non-point pollution project of Department of Soil Science, University of Wisconsin-Madison. Brian Hess, Department of Geology and Geophysics, UW-Madison, prepared the soil thin sections and helped to identify the key soil features under a microscope. The authors wish to express their sincere thanks to Dr. Janis Boettinger and three anonymous referees for their constructive comments on the original manuscript.

References

Assallay, A.M., I. Jefferson, C.D.F. Rogers, and I.J. Smalley. 1998. Fragipan formation in loess soils: Development of the Bryant hydrocons-olidation hypothesis. *Geoderma.* 83:1-16.

Bryant, R.B. 1989. Physical processes of fragipan formation. 141-150. *In N.E. Smeck and E.J. Ciolkosz (ed.) Fragipans: Their Occurrence, Classification, and Genesis.* SSSA Special Publication. No 24. Soil Science Society of America, Madison, WI.

Bullock, P., M.H. Milford and M.G.Cline. 1974. Degradation of argillic horizons in Udalf soils of New York State. *Soil Sci. Soc. Am. Proc.* 34:621-628.

Clayton, L. and J.W. Attig. 1997. *Pleistocene geology of Dane country, Wisconsin.* Wisconsin Geological and Natural History Survey. Bulletin 95. Madison, WI.

Franzmeier, D.P., L.D. Norton and G.C. Sterinhardt. 1989. Fragipan formation in loess of the

Midwestern United States. 69-97. *In* N.E. Smeck and E.J. Ciolkosz (*ed.*) *Fragipans: Their Occurrence, Classification, and Genesis.* SSSA Special Publication. No 24. Soil Science Society of America, Madison, WI.

Gee, G.W., and J.W. Bauder. 1986. Particle size analysis. 383-412. *In* A.Klute (ed.) *Methods of Soil Analysis; Part 1 Physical and Mineralogical Meth-ods (2nd edition).* ASA and SSSA, Madison, WI.

Habecker, M.A., K. McSweeney, and F.W. Madison. 1990. Identification and genesis of fragipans in Ochrepts of north central Wisconsin. *Soil Sci. Soc. Am. J.* 54: 139-146.

Harlan, P.W. and D.P. Franzmeier. 1977. Soil formation on loess in southwestern Indiana: I. Loess stratigraphy and soil morphology. *Soil Sci. Soc. Am. J.* 41:93-98.

Hesse, P.R. 1968. *A Textbook of Soil Chemical Analysis.* John Murray, London.

Innes, R.P. and D.J. Pluth. 1970. Thin section preparation using epoxy impregnation for petrographic electron probe analysis. *Soil Sci. Soc. Am. Proc.* 34:483-485.

Jha, P.P. and M.G. Cline. 1963. Morphology and genesis of a Sol Brun Acide with fragipan in uniform silty material. *Soil Sci. Soc. Am. Proc.* 27: 339-344.

Karanthanasis, A.D. 1987. Thermodynamic evaluation of amorphous aluminosilicate binding agents in fragipans of Western Kentucky. *Soil Sci. Soc. Am. J.* 51:819-824.

Karanthanasis, A.D. 1989. Solution chemistry of Fragipan-Thermodynamic approach to understanding fragipan formation. 113-139. *In* N.E. Smeck and E.J. Ciolkosz (*ed.*) *Fragipans: Their Occurrence, Classification, and Genesis.* SSSA Special Publication. No 24. Soil Science Society of America, Madison, WI.

Lindbo, D.L. and P.L.M. Veneman. 1989. Fragipans in the Northeastern United States. 11-31. *In* N.E. Smeck and E.J. Ciolkosz (*ed.*) *Fragipans: Their Occurrence, Classification, and Genesis.* SSSA Special Publication. No 24. Soil Science Society of America, Madison, WI.

McDaniel, P.A. and A.L. Falen. 1994. Temporal and spatial patterns of episaturation in a Fragixeralf landscape. *Soil Sci. Soc. Am. J.* 58:1451-1457.

Miller, M.B., T.H. Cooper, and R.H. Rust. 1993. Differentiation of an eluvial fragipan from dense till in northern Minnesota. *Soil Sci. Soc. Am. J.* 57: 787-796.

Mitchell, M-J. 1978. *Soil Survey of Columbia County,* Wisconsin. USDA-SCS. U.S. Gov. Print. Office, Washington, DC.

Nettleton, W.D., W.D. Daniels and R.J. McCracken. 1968. Two North Carolina coastal plain catenas: I Morphology and fragipan development. *Soil Sci. Soc. Am. Proc.* 32: 577-582.

Norton, L.D. 1986. Erosion-sedimentation in a closed drainage basin in northwest Indiana. *Soil Sci. Soc. Am.* J. 50: 209-213.

Park, S.J. and T.P. Burt. 1999. Identification of throughflow intensity using the distribution of secondary iron oxides in soils. *Geoderma,* 93:61-84.

Park, S.J., McSweeney, K. and Lowery, B. 2001 Identification of the spatial distribution of soils using a process-based terrain characterization. *Geoderma,* 103:249-272.

Ray, L.L. 1967. *An interpretation of profiles of weathering of the Peorian loess of western Kentucky.* U.S. Geol. Surv. Prof. Pap. 576-D:221-227.

Samuelson, J.R. 1999. Landscape position and crop sequence impact on surface runoff, drainage, and agriculture chemical leaching. Unpublished M.S. thesis. University of Wisconsin-Madison. 222p.

Schoeneberger, P. J., D. A., E. Wysocki, C. Benham and W. D. Broderson. 1998. *Field book for describing and sampling soils, Version 1.1.* Natural Resources Conservation Service, USDA, National Soil Survey Center, Lincoln, NE.

Smeck, N.E. and Ciolkosz, E.J. 1989b. Summary. 151-

153. *In* N.E. Smeck and E.J. Ciolkosz (ed.) *Fragipans: Their Occurrence, Classification, and Genesis*. SSSA Special Publication. No 24. Soil Science Society of America, Madison, WI.

Soil Survey Staff. 1984. *Procedures for collecting soil samples and methods of analysis for soil survey.* USDA-SCS Soil Surv. Invest. Rep. U.S. Gov. Print. Office, Washington, DC.

Soil Survey Staff. 1998. *Keys to Soil Taxonomy (8th edition).* United States Department of Agriculture, Natural Resources Conservation Service. U.S. Gov. Print. Office, Washington, DC.

Soil Survey Staff. 1999. *Soil Taxonomy: A Basic System of Soil Classification for Making and Interpreting Soil Surveys (2nd edition).* United States Department of Agriculture, Natural Resources Conservation Service. Agriculture Handbook, No. 436

Steinhardt, G.C. and D.P. Franzmeier. 1979. Chemical and mineralogical properties of the fragipans of the Cincinnati catena. *Soil Sci. Soc. Am. J.* 43:1008-1013.

Walker, P.H. and R.V. Ruhe 1968. Hillslope models and soil formation, II. Closed systems. *Transaction of 9th International Congress of Soil Science.* 4:561-568.

Witty, J.E. and E.G. Knox 1989. Identification, role in Soil Taxonomy, and worldwide distribution of fragipans. 1-10. *In* N.E. Smeck and E.J. Ciolkosz *(ed.) Fragipans: Their Occurrence, Classification, and Genesis.* SSSA Special Publication. No 24. Soil Science Society of America, Madison, WI.

Correspondence : Soo Jin Park, Department of Geography, College of Social Sciences, Seoul National University, Seoul 151-742, Korea(e-mail : catena@snu.ac.kr, phone : 02-880-9007)

교신 : 박수진, 151-742 서울시 관악구 신림동 산 16-1 서울대학교 사회과학대학 지리학과 (이메일: catena@snu.ac.kr, 전화: 02-880-9007)

Received May 11, 2006
Accepted June 18, 2006